HHS Public Access

Author manuscript

Neuroscience. Author manuscript; available in PMC 2023 May 01.

Published in final edited form as:

Neuroscience. 2023 May 01; 517: 105–116. doi:10.1016/j.neuroscience.2023.03.003.

Activation of parabrachial tachykinin 1 neurons counteracts some behaviors mediated by parabrachial CGRP neurons

Joe Arthurs[1,2], **Jordan Pauli**[1,2], **Richard D. Palmiter**[1,2]

[1]Department of Biochemistry, University of Washington, Seattle, 98195, United States

[2]Howard Hughes Medical Institute, University of Washington, Seattle, 98195, United States

Abstract

Many threats activate parabrachial neurons expressing calcitonin gene-related peptide ($CGRP^{PBN}$) which transmit alarm signals to forebrain regions. Most $CGRP^{PBN}$ neurons also express tachykinin 1 (Tac1), but there are also Tac1-expressing neurons in the PBN that do not express CGRP (Tac1+;CGRP− neurons). Chemogenetic or optogenetic activation of all $Tac1^{PBN}$ neurons in mice elicited many physiological/behavioral responses resembling the activation of $CGRP^{PBN}$ neurons, e.g., anorexia, jumping on a hot plate, avoidance of photostimulation; however, two key responses opposed activation of $CGRP^{PBN}$ neurons. Activating $Tac1^{PBN}$ neurons did not produce conditioned taste aversion and it elicited dynamic escape behaviors rather than freezing. Activating Tac1+;CGRP− neurons, using an intersectional genetic targeting approach, resembles activating all $Tac1^{PBN}$ neurons. These results reveal that activation of Tac1+;CGRP− neurons can suppress some functions attributed to the $CGRP^{PBN}$ neurons, which provides a mechanism to bias behavioral responses to threats.

Graphical Abstract

Correspondence to: Richard D. Palmiter, Box 357350, 1705 NE Pacific St., Seattle, WA 98195-7350, palmiter@uw.edu.

Ethical statement

I have read and have abided by the statement of ethical standards for manuscripts submitted to Neuroscience. I further certify that all experiments involving animals were conducted in accordance with the National Institute of Health Guide for the Care and Use of Laboratory Animals and were approved by the University of Washington Institutional Animal Care and Use Committee. I further attest that all efforts were made to reduce the number of animals used in experiments and their suffering.

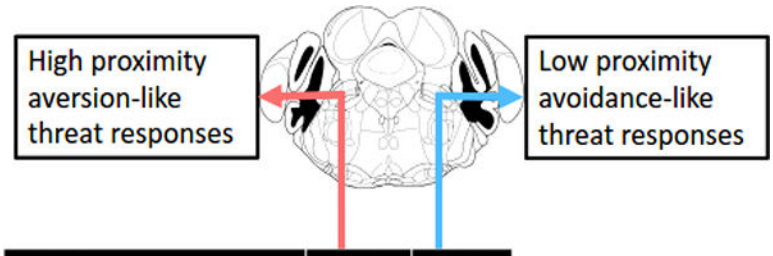

Behavior	CGRP^{PBN}	Tac1^{PBN}
Freezing	+	-
Conditioned taste aversion (CTA)	+	-
Jumping (hotplate)	+	+
Anorexia/Adipsia	+	+
Suppress CTA	-	+
Flight (locomotion)	-	+

Keywords

Conditioned taste aversion; escape; freezing; threat response; avoidance; INTRSECT

Introduction

The ability to identify and appropriately respond to threats is critical for survival. Threats to homeostasis may be subtle (e.g., the first hints of nausea signaling an impending bout of food poisoning) or startling (e.g., a pouncing predator) and require a range of behavioral responses for an animal to survive. Upon encountering a novel threat, animals will engage in innate defensive reactions. Learning associations between threats and the cues that predict them is essential for increasing long-term survival. The psychological literature has documented that animals form strong associations between biologically relevant predictive cues and the consequences they signal, a phenomenon called selective associations (e.g., Garcia & Koelling, 1966). However, the neural underpinnings of this phenomenon remain unclear. Candidate neural circuits need to involve the sensory processing of cues and threats and interface with circuits capable of generating behavioral responses. The parabrachial nucleus (PBN) is a likely node in these neural circuits because it is activated by a wide variety of threats and it has reciprocal connections with relevant forebrain regions, e.g., hypothalamus, extended amygdala, insular cortex, and brainstem.

Within the PBN, an astonishing range of threatening stimuli (e.g., somatic pain, visceral malaise, itch, and most strong sensory stimuli) activate calcitonin gene-related peptide (CGRP; encoded by the *Calca* gene) expressing neurons in the external lateral parabrachial nucleus (CGRP^{PBN}) neurons (Campos et al., 2018; Carter et al., 2013; Han et al., 2015; Kang et al., 2022). Photoactivation of these CGRP neurons induces freezing behavior, anxiety, autonomic arousal, and anorexia (Bowen et al., 2020; Campos et al., 2016; Carter et al., 2013). Furthermore, they are both necessary and sufficient for establishing conditioned

taste aversion (CTA) resulting from the pairing of a novel tastant with visceral malaise as well as forming fear-learning associations between external stimuli (e.g., tones) and somatic pain (e.g., foot shocks) (Chen et al., 2018; Han et al., 2015). This breadth of tuning and critical role in learning led to the characterization of $CGRP^{PBN}$ neurons as a general alarm system (Palmiter, 2018). Interestingly, fear and taste learning have long been viewed as distinct based on experiments showing that animals are adept at forming biologically relevant cue:threat associations such as taste:visceral malaise (interoceptive stimuli) or tone:shock pairing (exteroceptive stimuli) (Freeman & Riley, 2009; Garcia & Koelling, 1966; Gemberling et al., 1980; Gemberling & Domjan, 1982; Holland & Wheeler, 2009; Rusiniak et al., 1982) as compared with biologically mismatched associations (Delamater and Treit, 1988; Krane and Wagner, 1975). Thus, the fact that $CGRP^{PBN}$ neurons are necessary for both forms of learning is surprising, offering an opportunity to probe for other neuronal populations that interface with the general alarm signal of $CGRP^{PBN}$ neurons to generate appropriate behavioral responses to a particular threat.

Neurons within the PBN express many neuropeptides including CGRP, cholecystokinin, neurotensin, prodynorphin, pituitary adenylate cyclase-activating peptide, proenkephalin and tachykinin 1 (Pauli et al., 2022). Notably, most $CGRP^{PBN}$ neurons co-express tachykinin 1. Tachykinin 1 (*Tac1* gene), which encodes the precursor of both neurokinin A and substance P. Tac1 is widely expressed, often along with CGRP, in pain circuitry including dorsal root ganglia, spinal cord, trigeminal neurons and PBN (Edvinsson et al., 2021; Gutierrez-Mecinas et al., 2017). Recently $Tac1^{PBN}$ neurons were shown to be necessary and sufficient for generating escape responses, particularly jumping on a hot plate (Barik et al., 2018). Thus, we hypothesized that they might be involved in overriding the general alarm from $CGRP^{PBN}$ neurons from freezing into active avoidance (or escape) responses to threats involving somatic pain. To address this possibility, we infused adeno-associated viruses carrying recombinase-dependent genes in the PBN of transgenic mice to visualize the cell bodies and axonal projections of either Tac1, CGRP, or Tac1+;CGRP− as well as manipulate their activity. Using these methods, we provide evidence that activating Tac1 neurons biases defensive reactions towards escape-like behaviors and suppresses the formation of conditioned taste aversions generated either by activation of $CGRP^{PBN}$ neurons or malaise-inducing agents. This mechanism may provide a check on the general alarm and facilitate appropriate, defensive responses.

Experimental Procedures

Subjects

All subjects were adult male and female mice (P56-P140). $Tac1^{Cre/+}$ mice were obtained from Jackson Laboratory (stock #021877), and $Calca^{Cre}$ mice were generated and maintained as described by Carter et al. (2013) and are available at Jackson Laboratory (stock #033168). $Calca^{Flpo}$ (Arthurs, et al., *in revision*) mice were generated by our lab. All mice were backcrossed onto a C57BL/6J background for more than six generations. Genotypes of experimental mice were established using polymerase chain reaction. All studies involved mice of both sexes; no sex differences were noted but sample size was too small for statistical analysis. Mice were group-housed before surgery and singly housed

after recovering from surgery. They were housed on a 12-h light/dark cycle at 22°C with food and water available *ad libitum* unless otherwise noted in the experimental procedure. Experiments were conducted following guidelines from the NIH Guide for the Care and Use of Laboratory Animals, and all experimental procedures were approved by the University of Washington Institutional Animal Care and Use Committee.

Viral tools and production

The FLP recombinase-dependent AAV1-EF1α-frtDIO-mCherry virus was purchased from AddGene (stock #114471). Plasmids for pAAV-Ef1a-Cre_{ON}/$FLPo_{OFF}$-ChR2:eYFP (Fenno et al., 2014) were acquired from Addgene. pAAV-Ef1α-DIO-ChR2:YFP and pAAV-hSyn-DIO-YFP DNA plasmids were provided by K. Deisseroth (Stanford University).The FLP recombinase-dependent pAAV-hSyn-frtDIO-mCherry plasmid was prepared in house. pAAV-Ef1α-DIO-Synaptophysin:mCherry DNA plasmid was generated from pAAV-Ef1α-DIO-Synaptophysin:GFP (Roman et al., 2016). pAAV-hSyn-DIO-hM3Dq:YFP DNA plasmid was generated from pAAV-hSyn-DIO-hM3Dq:mCherry (#44361) DNA plasmid from AddGene. Some viruses were prepared in-house, in which case HEK cells were transfected with each plasmid plus pDG1 (AAV1 coat stereotype plus helper genes); viruses were purified by sucrose and CsCl-gradient centrifugation steps, re-suspended in 0.1 M phosphate-buffered saline (PBS) at approximately 10^{13} viral particles/ml, aliquoted, and stored at −80°C.

Stereotaxic Surgery

Mice were anesthetized with isoflurane (1–4%), treated with ketoprofen (5 mg/kg, IP), and secured in a stereotaxic frame (Kopf Model 1900). An incision site on the scalp was prepared by removing hair and cleaning the skin with alternating washes of betadine and ethanol. The cranial sutures were exposed via a midline incision allowing visualization of landmarks on the skull. A drill mounted to the stereotaxic frame was used to drill holes in the skull overlying the PBN. Targeting coordinates were referenced from bregma for AP and ML coordinates and dura for the DV coordinate and were as follows: PBN fibers and virus (AP: −4.8, ML: ±1.4, and DV: −3.3 for virus and −3.0 for fiber optic cannulae). Virus (200–300 nL) was injected bilaterally targeting the PBN using a glass capillary micropipette attached to a Nanoject II (Drummond Scientific). An additional hole was drilled in the skull to allow the anchoring of a bone screw (FST Item No. 19101–00). The fiber optic cannula and the bone screw were cemented to the skull with cyanoacrylate hardened with dental acrylic monomer. A headcap reinforcing all implants and filling the incision was formed from dental acrylic and the ends of the wound were secured with suture. Isoflurane anesthesia was discontinued, and mice were allowed to recover for at least 3 weeks before undergoing experiments.

Histology and Microscopy

Mice from behavioral experiments received a fatal overdose of pentobarbital (Euthasol®, 270 mg/kg, IP, Merck) and were perfused transcardially with ice-cold PBS followed by 4% paraformaldehyde in phosphate-buffered saline. Brains were post-fixed for 2–24 hours at 4°C depending on the quality of the perfusion and then cryoprotected in 30% sucrose, frozen in TissuePlus OCT (ThermoFisher), and stored at −80°C before sectioning (15–35μm) on a

cryostat (Leica Microsystems). For *in-situ* hybridization, fresh frozen brains were sectioned at 15–20 μm and directly mounted to glass slides whereas for all other purposes tissue was sectioned at 30 μm and collected into cold PBS for immunohistochemical processing and wet mounting on glass slides. All images were collected using either a Keyence BZ-X710 microscope or Olympus Fluoview FV-1200 confocal microscope. Images were minimally processed for brightness and contrast.

Immunohistochemistry

For immunohistochemical experiments, PBS with 0.2% Triton X-100 (PBST) was used for three 5-min washes before 1-hour incubation in a blocking solution of 3% normal donkey serum in PBST. Sections were then incubated in the primary antibody at 4°C overnight. Primary antibodies used were rabbit anti-Fos (1:2000; Abcam, ab190289), rabbit anti-DsRed (1:000, Takara 632496), chicken anti-GFP (1:10000, Abcam, ab13970), mouse anti-CGRP (1:1000, Abcam, ab81887). Primary antibody was removed with three 5-min washes in PBS followed by incubation for 1 hour in PBS with secondary antibodies including donkey anti-rabbit IgG Cy5, donkey anti-chicken IgG AlexaFluor 488, donkey anti-rabbit IgG Alexa Fluor 594, and donkey anti-mouse IgG Alexa Fluor 594 (1:500–1:1000, Jackson ImmunoResearch).

Fluorescent *in-situ* hybridization

Brains were collected from mice anesthetized with isoflurane and euthanized via decapitation. After extraction, brains were frozen for approximately 60 sec in 2-methylbutane cooled with Dry Ice to −30 °C. Samples were stored at −80°C until cut into 20-μm sections on a cryostat. Sections were processed using RNAscope Multiplex Fluorescent Assay (version 1) to label *Tac1* (Atto 647) and *Calca* (AF 488) RNA according to manufacturer instructions (Advanced Cell Diagnostics).

BioDAQ consummatory behavior

Mice were individually housed in BioDAQ recording chambers (Research Diets) and acclimated to consuming food or water from the monitored hopper apparatus. Animals were habituated for at least 7 days before experimental manipulation or either food or water intake. Cumulative food and water intake during the dark cycle, was analyzed via BioDAQ Viewer. Clozapine-N-oxide (CNO) was injected (1 mg/kg, IP) 30 min before the start of the dark cycle to activate neurons expressing hM3D(Gq).

Hot plate

Mice were injected with CNO (1 mg/kg, IP) 30 min before being placed on a 55°C hot plate (Bioseb) for 30 sec. Behavior on the hotplate was recorded and video was scored offline for latency to lick a hind paw or jump, as well as the number of times animals, jumped up off the hotplate.

Small Arena

Mice were prepared for photostimulation by connecting the implanted fiber-optic cannulae to a blue-light laser via a fiber-optic cable before being placed in a well-lighted

arena (10×10 cm). After habituating to the experimental setup for 1 min, mice were photostimulated (30 Hz, 10 sec) twice with a 1-min interstimulus interval. Video of the behavioral responses to photostimulation was scored offline. Freezing was defined as rigid uninterrupted immobility that was usually terminated by the initiation of head movement. Locomotion was defined as a continuous period of forward movement.

Big Arena

Mice were prepared for photostimulation by connecting the implanted fiber-optic cannulae to a blue-light laser via a fiber optic cable before being placed in a well-lighted arena (10×50 cm). Mice were habituated to the apparatus for 5 min before undergoing two bouts of photostimulation (30 Hz, 10 sec) separated by a 1-min interstimulus interval. On another day, a partial low wall (12 cm) extending 7.5 cm into the arena was added creating a small hide area that was 10 cm square with an entrance of about 2.5 cm and a small, shaded corner. The habituation period was extended to 10 min to encourage animals to explore outside the hide area. The laser was activated for 10 sec (30 Hz) when mice were at the end of the arena opposite the hide area. Behavioral responses were recorded and scored as for the small arena test with the addition that time spent within the hide box was also quantified when applicable.

Real-time place conditioning

Mice were prepared for photostimulation as above and placed into a two-chamber real-time place conditioning apparatus. Each chamber measured 28 cm by 28 cm with distinct visual cues (i.e., vertical versus horizontal stripes). Photostimulation (15 Hz) on one side of the apparatus began after an initial 5-min baseline period to assess initial preferences. 15-Hz photostimulation was selected so that movement phenotypes (i.e., freezing, jumping) would not interfere with their ability to move freely between chambers.

Conditioned taste aversion

Our standard conditioned taste aversion paradigm has been described (Chen et al., 2018). Mice were acclimated to individual housing in custom cages with two ports for attaching drinking tubes and then adapted to scheduled water access 30 min in the morning and 1 hour in the afternoon for three days. Intake was recorded in grams and converted to milliliters. The three conditioning trials consisted of pairing 30 min of 5% sucrose access with an injection of CNO (1 mg/kg, IP) as the unconditioned stimulus followed by scheduled water access that afternoon and the following day. Finally, animals were given a 2-bottle test consisting of 30-min access to both sucrose and water. For optogenetic CTA experiments, the unconditioned stimulus was 30 min of optical stimulation via a blue laser (30 Hz, 3-sec on 2-sec off). To examine the capacity of $Tac1^{PBN}$ neuronal stimulation to attenuate a LiCl-induced CTA, mice were administered CNO (1 mg/kg, IP) immediately after 30-min access to 0.2% saccharin and 30 min before being administered LiCl (180 mg/kg, IP) on each of two conditioning trials. Finally, animals were given a 2-bottle test consisting of 30-min access to both saccharin and water. For this experiment we made several changes to our standard CTA paradigm. We extended the interstimulus interval between the CS and US for CNO to be maximally effective when the US was administered. We also found that sucrose was ineffective as a CS with this longer interstimulus interval and switched

to saccharin, as it evokes a stronger neophobic reaction (e.g., Kronenberger and Medioni, 1985).

Data analysis

All data were analyzed using OriginPro (OriginLab) software to conduct two-way repeated measures ANOVAs, one-way ANOVAs, or t-tests as appropriate with Fisher post hoc tests. Notably, due to software limitations, only the first ten hours (out of 12 total) of cumulative intake were analyzed in two-way repeated measures ANOVAs for experiments examining food and water intake during the dark cycle.

Results

Chemogenetic activation of either Tac1^{PBN} or CGRP^{PBN} neurons causes anorexia, adipsia, and jumping on a hotplate.

Barik et al. (2018) described a role for parabrachial Tac1-expressing neurons in mediating escape behaviors to noxious stimuli, including a hot plate and inflammatory pain. Their experiments using chemogenetic activation (Armbruster et al., 2007) indicated that there are at least two distinct populations of Tac1 neurons in the PBN; those that project to forebrain regions such as the central nucleus of the amygdala (CeA) and those that project to the reticular formation in the medulla, referred to as MdD. Non-selective inactivation of Tac1 neurons in the PBN suppressed escape behaviors, while selective activation of the projection to MdD (but not the CeA projection) promoted jumping behavior on the hot plate. They compared the results of activating hM3Dq in Tac1^{PBN} neurons with activating neurotensin (*Nts*) expressing PBN neurons (NTS^{PBN}) or CGRP^{PBN} neurons and concluded that only activation of the Tac1 neurons promoted escape behaviors. They reported minimal *Calca* and *Tac1* mRNA overlap in the PBN, with *Tac1* being expressed in the lateral PBN and *Calca* in the external lateral PBN. However, the Allen Mouse Brain Atlas reveals robust *Tac1* expression in the external lateral region like *Calca* and *Nts*, and we have shown by scRNA-Seq and RiboTag approaches that *Calca* and *Tac1* are extensively co-expressed in the external lateral PBN (Pauli et al., 2022).

The co-expression of *Calca* and *Tac1* expression raised concerns about the unique role of Tac1^{PBN} neurons in mediating escape behaviors. We bilaterally injected AAV1-DIO-hM3Dq:YFP (or AAV1-DIO-YFP as control) into the PBN of either *Tac1*^{Cre} or *Calca*^{Cre} mice, administered CNO at 1 mg/kg to selectively activate the neurons, and compared the behavioral responses (Fig. 1A–C). Activating either population of neurons just before the dark period (when mice eat and drink the most) suppressed food and water intake for several hours compared to YFP controls; intake gradually recovered by 12 hr (Fig. 1D, F). Specifically, a two-way repeated measures ANOVA of food intake in Tac1 mice detected a significant main effect of Group ($F(1,11) = 18.38$ $p < .01$), Time ($F(1,9) = 194.60$, $p < .0001$), and Interaction ($F(1,9) = 12.08$, $p < .0001$). Analysis of food intake in CGRP mice revealed a significant main effect of Group ($F(1,10) = 6.50$ $p < .05$), Time ($F(1,9) = 68.16$, $p < .0001$), and an Interaction ($F(1,10) = 3.15$, $p < .01$). The effect of hM3Dq activation in CGRP^{PBN} neurons was expected based on previous research (Carter et al., 2013); the result of activating Tac1-hM3^{PBN} neurons had not been reported but could be

predicted based on co-expression of *Tac1* with *Calca*. Water intake by the two groups of mice was similarly suppressed by activating hM3Dq with CNO in either Tac1-hM3^{PBN} or CGRP-hM3^{PBN} neurons (Fig. 1E, G), which is expected because mice consume most of their water intermittently while eating. For Tac1 water intake, a two-way repeated measures ANOVA showed a trending main effect of Group ($F(1,11) = 4.83$, $p = 0.05018$, and a significant main effect of Time ($F(1,9) = 93.92$, $p < .0001$), and an Interaction ($F(1,11) = 9.17$. $p < .0001$). For CGRP water intake, there was a significant main effect of Group ($F(1,10) = 5.522$, $p < .05$), Time ($F(1,9) = 65.22$, $p < .0001$), and an Interaction ($F(1,10) = 2.437$, $p < .05$).

To compare the responses to painful stimuli, a novel cohort of mice was administered CNO and then 30 min later placed on a 55°C hot plate for 30 sec. The latency to respond (10–15s) after being placed on the hot plate was the same for Tac1-hM3^{PBN} ($t(10) = -1.340$, $p > .05$) and CGRP-hM3^{PBN} ($t(12) = -0.804$, $p > .05$) neurons compared to YFP controls (Fig. 1H, J). However, the nature of the response was different. The initial response of YFP controls was always licking the hind paw, whereas activation of either Tac1 or CGRP mice resulted in jumping. Specifically, the majority of Tac1-hM3^{PBN} ($t(5) = 4.757$, $p < .01$) or CGRP-hM3^{PBN} ($t(12) = -4.547$, $p < .001$) jumped (i.e., escape-like behavior) as the initial response (5 of 6 for Tac1-hM3 and 5 of 7 for CGRP-hM3), whereas only two of the YFP mice jumped during the entire test and never as the initial response (Fig. 1I, K). The number of jumps by the Tac1-hM3^{PBN} mice reported here is like that reported by Barik et al. (2018), but unlike their results, the CGR-hM3^{PBN} mice jumped just as much. Jumping on the hot plate by the CGRP-hM3^{PBN} mice is consistent with our prior results showing that inactivation of CGRP^{PBN} neurons with tetanus toxin blocked jumping (Han et al., 2015) and photoactivation of axon terminals of CGRP-ChR2^{PBN} neurons in the CeA promoted jumping (Bowen et al., 2020). We conclude that jumping in response to thermal pain is not an exclusive phenotype of Tac1^{PBN} projections to the MdD.

Optogenetic activation of either Tac1^{PBN} or CGRP^{PBN} neurons elicits opposing defensive behaviors.

The previous results based on chemogenetic technology reveal that activation of either Tac1^{PBN} or CGRP^{PBN} neurons resulted in similar behaviors; however, the degree of activation of hM3Dq with CNO is less than what can be achieved by photoactivation of channelrhodopsin. Robust (30 Hz, 15 mW) photoactivation of CGRP-ChR2^{PBN} neurons results in profound freezing behavior in which mice remain in awkward positions and resist moving even when prodded (Bowen et al., 2020). When we compared the photoactivation of Tac1-ChR2^{PBN} and CGRP-ChR2^{PBN} neurons, the responses of the mice were distinctly different. AAV1-DIO-ChR2:YFP (or YFP only as control) was injected into the PBN of *Tac1*^{Cre} or *Calca*^{Cre} mice, and fiber-optic cannulas were implanted above the PBN (Fig. 2A–C). After several weeks for viral expression, mice were placed in a small (10 × 10 cm) arena and photoactivated at 30 Hz (10 mW) for three 10-sec intervals. The percent time freezing ($F(2,11) = 507.27$, $p < .0001$) or locomoting ($F(2,11) = 210.48$, $p < .0001$) during stimulation was assessed from video recordings. As predicted, photoactivation of CGRP-ChR2^{PBN} neurons resulted in freezing (i.e., immobility of the head and body with no locomotion) with negligible locomotion; in contrast, photoactivation of Tac1-ChR2^{PBN}

neurons resulted in bouts of rapid locomotion indicative of escape behavior with no freezing compared to the YFP control mice ($p < .05$) (Fig. 2D, E). When this experiment was repeated using a larger arena (10 × 50 cm) that would allow more room for locomotion, the results were similar but less dramatic; photoactivation of CGRP-ChR2^{PBN} neurons promoted freezing ($F(2,11) = 13.599$, $p < .01$), although only 70% of the time (Fig. 2F), while again photoactivation of Tac1-ChR2^{PBN} neurons only promoted locomotion ($F(2,11) = 15.755$, $p < .001$); YFP controls also moved more in the larger arena the (Fig. 2G). In the third repeat of this experiment, a partial wall was installed 10 cm from one end of the larger arena to create an accessible "hide" area. Photoactivation of the CGRP-ChR2^{PBN} neurons at the end opposite to the hide area still resulted in prolonged freezing ($F(2,11) = 273.68$, $p < .0001$) (Fig. 2H), but after activation of all Tac1-ChR2^{PBN} neurons the mice spent more time locomoting compared to YFP or CGRP-ChR2^{PBN} ($F(2,11) = 7.379$, $p < .01$) (Fig. 2I). A one-way ANOVA revealed only a trending effect for time spent in the "hide" area ($F(2,11) = 3.244$, $p = 0.078$)(Fig. 2J). However, it is interesting that CGRP^{PBN} stimulated mice spent no time in the "hide" area. These results reveal that robust activation of Tac1-ChR2^{PBN} neurons promotes escape like behaviors – running if there is no choice but hiding some of the time if that is possible – whereas the CGRP-ChR2^{PBN} mice freeze regardless of the options available.

Distinct populations of neurons co-express *Tac1* and *Calca* versus neurons that express *Tac1* without *Calca*.

The results in Fig. 1 are compatible with *Tac1* and *Calca* being co-expressed; however, with more intense stimulation, some phenotypes are distinct (Fig. 2), which is difficult to reconcile with strict co-expression. We used RNAscope *in-situ* hybridization to locate the co-expressing neurons and ascertain whether there are neurons that express *Tac1* without *Calca* (Tac1+;CGRP−) and, if so, where they reside in the PBN. The RNAScope experiments revealed extensive co-expression of *Tac1* and *Calca* in the external lateral region of the PBN as expected; however, many Tac1+;CGRP− neurons were present in other subdivisions of the PBN, including dorsal lateral, superior lateral, central lateral and even medial regions (Fig. 3). We have reported elsewhere that the majority of *Tac1* neurons (~55%) do not co-express *Calca* (Arthurs et al., *in revision*; see also Pauli et al., 2022).

Activation of Tac1^{PBN} neurons suppresses conditioned taste aversion.

Pairing access to a novel food with activation of CGRP^{PBN} neurons, using either hM3Dq and CNO or photoactivation of ChR2, suppresses the consumption of that food on subsequent exposure – a phenomenon called conditioned taste aversion (CTA) (Carter et al., 2015; Chen et al., 2018). We compared CTA responses of mice expressing hM3Dq, or YFP controls, in Tac1-hM3^{PBN} or CGRP-hM3^{PBN} neurons (Fig. 4A). We paired 30-min access to 5% sucrose in water-deprived mice with CNO on two separate days, followed two days later by giving the mice a choice of sucrose or water. Tac1-hM3^{PBN} mice failed to learn a CTA despite the overlap between neurons expressing *Tac1* and *Calca* ($t(9) = 1.116$, $p = .293$) (Fig. 4B). As expected, mice with activation of CGRP-hM3^{PBN} neurons had a low preference for sucrose, indicative of a CTA ($t(10) = 4.738$, $p < .001$) (Chen et al., 2108) (Fig. 4C). Due to the overlap between Tac1^{PBN} and CGRP^{PBN} neurons, these results suggest that activating Tac1^{PBN} neurons overrides the effect of activating CGRP^{PBN}

neurons and prevents the establishment of a taste aversion. Alternatively, activating the subset neurons that express both Tac1 and CGRP (~45%) may be insufficient to establish a CTA. In a second cohort of mice, we tested whether activating Tac1^{PBN} neurons could attenuate the formation of a CTA based on visceral malaise produced by LiCl. *Tac1^{Cre}* mice were injected with AAV-DIO-hM3Dq-YFP or AAV-DIO-YFP as control. In third cohort of mice, we used a similar CTA paradigm except for access to the saccharine (the conditioned stimulus; CS) was followed immediately with an injection of CNO (1 mg/kg, IP) and then 30 min later by injection of LiCl (the unconditioned stimulus, US; 180 mg/kg, IP) a classic CTA-inducing agent. Activation of Tac1-hM3^{PBN} neurons significantly attenuated LiCl-mediated CTA compared to YFP controls ($t(13) = -3.638$, $p < .01$) (Fig. 4D). Next, in a fourth cohort of mice, we compared the CTA responses of mice expressing ChR2 in four different groups of mice (Fig. 4E): Tac1^{PBN} neurons (*Tac1^{Cre}*), Tac1+;CGRP− neurons (*Tac1^{Cre}::Calca^{FLPo}*, Fig. 4F), Tac1 and CGRP neurons (*Tac1^{Cre}::Calca^{Cre}* mice, Fig. 4G) and CGRP^{PBN} (*Calca^{Cre}*) neurons . We paired 30-min access to sucrose in water-deprived mice with photoactivation of ChR2 (30 Hz, 3 sec on, 2 sec off) on two separate days, followed two days later by giving the mice a choice of sucrose or water. As expected, the CGRP-ChR2^{PBN} mice developed a CTA and avoided the sucrose, whereas none of the other groups developed a CTA and continued to prefer sucrose ($F(3,16) = 15.885$, $p < .0001$) (Fig. 4H). Thus, like the suppression of freezing behavior, activation of Tac1^{PBN} neurons blocks or attenuates the CTA generated either by activating CGRP^{PBN} neurons or classical LiCl-induced visceral malaise. Activation of CGRP-ChR2^{PBN} neurons is aversive and results in a place aversion in a real-time place preference paradigm (RTPP) (Bowen et al., 2020). We asked whether activation of Tac1+;CGRP− neurons would also generate a place aversion in an RTPP paradigm. Photoactivation at 15-Hz of mice from the Tac1+;CGRP− mice from the CTA experiment produced a profound place aversion in an RTPP paradigm and the effect remained after stimulation was discontinued ($F(2,15) = 19.287$, $p < .001$) (Fig. 4I).

Parabrachial Tac1 and CGRP neuron axon projections have distinct post-synaptic targets.

To accurately compare the projections of Tac1^{PBN} and CGRP^{PBN} neurons, we co-injected AAV1-DIO-YFP and in *Tac1^{Cre}::Calca^{Flpo}* mice (n = 3). Fig. 5A–D show the expression of both fluorescent proteins at 4 coronal (rostral to caudal) levels of the PBN, revealing distinct expression patterns. There is substantial overlap of the fluorescent proteins only in the external lateral PBN. Based on labelling we could divide neurons into Tac1+;CGRP− (green), Tac1/CGRP (yellow), and CGRP+;Tac1− (red).

We saw projections from all three populations in each downstream target structure. However, this approach allowed us to discern subtle differences in the axon projections within target brain regions. For example, there were green Tac1+;CGRP− fibers in the ventral part of the lateral septum (Fig. 5E) and insular cortex (Fig. 5F), whereas red fibers from CGRP neurons were rare. Within the bed nucleus of the stria terminalis (BNST) there was a mixture of fiber patterns with most co-labeled fibers in the oval subdivision (BNSTov) with a more distinct Tac1+;CGRP− and CGRP+;Tac1− fibers in the ventral portion of the BNST (BNSTv) (Fig. 5G). In the thalamus there were few Tac1+;CGRP− fibers but CGRP-only fibers were present in several thalamic nuclei including the nucleus of reuniens (Re) and rhomboid nucleus (Rh). There were some co-labeled and Tac1+;CGRP− fibers in

the region of the rostral border of parasubthalamic nucleus (Fig. 5H). Within the amygdala, Tac1+;CGRP− fibers extended more into the lateral and medial regions of the rostral CeA than the CGRP+;Tac1− fibers. However, there were also many co-labeled fibers in the lateral capsular CeA (CeC) (Fig. 5I). A less distinct partial segregation of colors was apparent in the caudal CeA, VPMpc, and PSTN (Fig. 5 J, K), with green and red fibers in proximity but little co-expression. There were strong Tac1+;CGRP− fibers in the posterior portion of the basolateral amygdala (Fig. 5L). Within the medullary reticular nucleus dorsal part (MdD), which was a focus of the Barik et al (2017) study, we see diffuse green and red fibers indicating widespread projections from both Tac1+;CGRP− and CGRP+;Tac1− neurons with few if any yellow fibers noted (Fig. 5 M, N). These results suggest that even within the same brain region distinct post-synaptic cells are likely to innervated by the Tac1+;CGRP− versus the Tac1/CGRP co-expressing neurons.

Discussion

While Tac1 and CGRP are co-expressed in the external lateral PBN, there are many neurons in the PBN that express Tac1 without CGRP. The $CGRP^{PBN}$ neurons are activated by a wide variety of sensory stimuli, somatic and visceral threats, as well as cues that predict harm; consequently, they appear to serve as a general alarm. A common response to virtually all threats is transient suppression of non-essential behaviors to facilitate attention being directed towards the immediate threat. For example, animals will cease consummatory behaviors upon sensory detection of potential predators and either flee, freeze or attack depending on the proximity of the predator (Apfelbach et al., 2005; Blanchard et al., 2005; Bolles, 1970; Lenzi et al., 2022; Narushima et al., 2022). Beyond this alarm role, $CGRP^{PBN}$ neurons play an important role in learning to avoid future threats; they convey the unconditioned stimulus (US) in classical conditioning experiments. Pairing chemogenetic or optogenetic activation $CGRP^{PBN}$ neurons with innocuous cues results in conditioned responses, while inactivation of these neurons suppresses the ability to learn to avoid natural threats (Bowen et al., 2020; Campos et al., 2016, 2018; Chen et al., 2018; Han et al., 2015; Palmiter, 2018). An effective alarm system needs a mechanism to discern the nature of the threat to allow an appropriate response. The $CGRP^{PBN}$ neurons project their axons to several forebrain regions, so perhaps their US signals converge with sensory conditioned stimuli (CS) in different post-synaptic neurons to elicit appropriate responses. Alternatively, while most threats activate $CGRP^{PBN}$ neurons, they may also activate other neurons within the PBN as well, such that the constellation of neurons that are activated dictates appropriate responses. This idea is consistent with the observation that while most threats activate Fos in $CGRP^{PBN}$ neurons, Fos is also expressed in many other undefined PBN neurons as well (e.g., Carter et al., 2013; Chen et al., 2022; Lee et al., 2021). We show that activation of Tac1+;CGRP− neurons can suppress some functions of $CGRP^{PBN}$ neurons and thereby preclude the freezing behavior or taste conditioning that would result from activating only the $CGRP^{PBN}$ neurons.

The co-expression of Tac1 and CGRP in the external lateral PBN explains the nearly identical effects of chemogenetically activating $Tac1^{PBN}$ and $CGRP^{PBN}$ neurons in the generation of anorexia and adipsia as well as biasing behavioral responses on a hot plate toward active escape (i.e., jumping) rather than the typical paw licking behavior seen in

control animals. However, this similarity highlights the remarkable differences observed after the optogenetic activation of these populations. Optogenetic stimulation of $CGRP^{PBN}$ neurons generated robust freezing behavior as previously reported (Bowen et al., 2020); however, stimulation of $Tac1^{PBN}$ neurons had an opposite effect causing robust locomotion behavior, while animals actively avoid stimulation of either neuronal population in the RTPP assay (Bowen et al., 2020). We assume that activation of hM3Dq with CNO amplifies ongoing signaling events whereas photoactivation may provide an extra (unnatural) boost in activity to the Tac1+;CGRP− neurons, allowing them to suppress the function of $CGRP^{PBN}$ neurons and prevent freezing behavior. We predict that when a predator is detected at a distance, the $CGRP^{PBN}$ neurons are initially activated to promote freezing but as a predator approaches the Tac1+;CGRP− neurons are activated, which suppresses the activity of the $CGRP^{PBN}$ neurons and promotes active escape-like behaviors.

Remarkably, chemogenetic activation of $Tac1^{PBN}$ neurons failed to produce CTA in the same behavioral paradigm that resulted in robust CTA after stimulating $CGRP^{PBN}$ neurons. We used $Tac1^{Cre}$::$Calca^{Flpo}$ mice along with dual-recombinase INTRSECT viruses to express ChR2 in Tac1+;CGRP− neurons and found that pairing sucrose with activation of these neurons failed to generate a CTA. Furthermore, chemogenetic activation of $Tac1^{PBN}$ neurons attenuated a LiCl-induced CTA. Because $CGRP^{PBN}$ neurons are activated by visceral malaise induced by lithium chloride, lipopolysaccharide, or GDF15 (Carter et al., 2013; Sabatini et al., 2021) and are necessary for establishing a CTA (Chen et al., 2018), we predict that the Tac1+;CGRP− neurons can suppress the function of $CGRP^{PBN}$ neurons to prevent CTA. This inhibition could be due to preferential activation of Tac1+;CGRP− neurons under some conditions (e.g., somatic pain) coupled with an indirect, negative-feedback circuit onto $CGRP^{PBN}$ neurons or their post-synaptic targets. Several possible negative-feedback circuits can be envisioned. Because Tac1+;CGRP− and $CGRP^{PBN}$ neurons are glutamatergic (express Vglut2) the circuit needs to include intervening inhibitory neurons (Pauli et al., 2022). One possibility is a short-loop within the PBN: Tac1+;CGRP− → GABA interneuron → CGRP. Alternatively, there could be a long-loop, inhibitory circuit from post-neurons, e.g., in CeA or BNST, regions that are known to have GABAergic projections to the PBN (Bartonjo and Lundy, 2022; Cai et al., 2014; Douglass et al., 2017; Jia et al., 2005; Lundy, 2020; Luskin et al., 2021; Raver et al., 2020). We show that both $CGRP^{PBN}$ and $Tac1^{PBN}$ neurons project axons to the CeA and BNST but their anatomical destinations within these regions differ. For example, the CGRP terminals are largely restricted to the lateral capsule of the CeA, whereas the Tac1 terminals extend into the lateral and medial region, which are presumably from the Tac1+;CGRP− neurons. RNAscope *in situ* hybridization studies reveal *Calcrl* mRNA (encodes CGRP receptor) in the lateral capsule and *Tacr1* mRNA (encodes substance P receptor) in lateral/medial regions of the CeA, and both populations of neurons are GABAergic (Bowen et al., 2023). These observations suggest that GABAergic, *Tacr1*-expressing, neurons in the CeA that are activated by $Tac1^{PBN}$ neurons could either project back to the PBN to inhibit $CGRP^{PBN}$ neurons or inhibit *Calcrl*-expressing neurons in the CeA. Additional experiments will be needed to examine these hypothetical feedback circuits.

Overall, these experiments reveal both the value and dangers of studying the behavioral consequences of activating specific neuronal populations. The value comes from being able

to describe what activating or inhibiting specific neurons can do. However, the danger is that those specific neurons may never be selectively activated; consequently, activating the ensemble of neurons is more physiological. While there are now several ways to trap and manipulate neuron ensembles (Franceschini et al., 2020; Guenthner et al., 2013), understanding the intercellular mechanisms involved depends on knowing the individual roles of all the neurons in the ensemble.

Acknowledgments

We thank Susan Phelps for animal husbandry. We also thank members of the Palmiter and Zweifel laboratories for their feedback on this project. This work was supported in part by the National Institutes of Health R01-DA024908 (RDP).

Abbreviations

ac	anterior commissure
AP	anterior-posterior axis
BLA	basolateral amygdala
BLP	basolateral amygdaloid nucleus posterior part
BNST	bed nucleus of the stria terminalis
BNSTov	bed nucleus of the stria terminalis oval nucleus
BNSTv	bed nucleus of the stria terminalis ventral nucleus
Calca	gene that encodes calcitonin-gene related peptide
CeA	central nucleus of the amygdala
CeC	Central nucleus of the amygdala lateral capsular part
CeL	central nucleus of the amygdala lateral part
CeM	central nucleus of the amygdala medial part
CGRP	calcitonin gene-related peptide
CM	central medial nucleus of the thalamus
CNO	clozapine-N-oxide
CS	conditioned stimulus
CTA	conditioned taste aversion
DV	dorsal-ventral axis
IP	Intraperitonea
GDF15	growth differentiation factor 15

IC	insular cortex
IMD	intermediodorsal nucleus of the thalamus
LiCl	lithium chloride
LSV	lateral septal nucleus ventral part
LSI	lateral septal nucleus intermediate part
MdD	medullary reticular nucleus dorsal part
ML	medial-lateral axis
MS	medial septal nucleus
NTS	neurotensin
PBN	parabrachial nucleus
PBS	phosphate buffered saline
PSTN	parasubthalamic nucleus
PVT	paraventricular nucleus
Re	reuniens thalamic nucleus
Rh	rhomboid thalamic nucleus
scp	superior cerebellar peduncle
SH	septohippocampal nucleus
Tac1	tachykinin 1
Tacr1	tachykinin 1 receptor
US	unconditioned stimulus
VPMpc	ventroposteriormedial thalamic nucleus parvocellular part

REFERENCES

Apfelbach R, Blanchard CD, Blanchard RJ, Hayes RA, McGregor IS, The effects of predator odors in mammalian prey species: A review of field and laboratory studies. Neurosci. Biobehav. Rev, 29 (2005) pp. 1123–1144. 10.1016/j.neubiorev.2005.05.005 [PubMed: 16085312]

Armbruster BN, Li X, Pausch MH, Herlitze S, Roth BL, Evolving the lock to fit the key to create a family of G protein-coupled receptors potently activated by an inert ligand. Proc. Natl. Acad. Sci. U. S. A. 104 (2007) pp. 5163–5168. 10.1073/pnas.0700293104 [PubMed: 17360345]

Barik A, Thompson JH, Seltzer M, Ghitani N, Chesler AT, A Brainstem-Spinal Circuit Controlling Nocifensive Behavior. Neuron 100 (2018), pp. 1491–1503 10.1016/j.neuron.2018.10.037 [PubMed: 30449655]

Bartonjo JJ, Lundy RF, Target-specific projections of amygdala somatostatin-expressing neurons to the hypothalamus and brainstem. Chem. Senses 47 (2022), bjac009. 10.1093/chemse/bjac009 [PubMed: 35522083]

Blanchard DC, Blanchard RJ, Griebel G, Defensive responses to predator threat in the rat and mouse. Curr. Protoc. Neurosci. 8 (2005) pp. 8–19.

Bolles RC, Species-specific defense reactions and avoidance learning. Psychol. Rev. 77 (1970) pp. 32–48. 10.1037/h0028589

Bowen AJ, Chen JY, Huang YW, Baertsch NA, Park S, Palmiter RD, Dissociable control of unconditioned responses and associative fear learning by parabrachial CGRP neurons. eLife 9 (2020) 10.7554/eLife.59799

Bowen AJ, Huang YW, Chen JY, Pauli JL, Campos CA, Palmiter RD. Topographic representation of current and future threats in the mouse nociceptive amygdala. Nat Commun. 2023 Jan 13;14(1):196. doi: 10.1038/s41467-023-35826-4. [PubMed: 36639374]

Cai H, Haubensak W, Anthony TE, Anderson DJ, Central amygdala PKC-δ+ neurons mediate the influence of multiple anorexigenic signals. Nat. Neurosci. 17 (2014) pp. 1240–1248. 10.1038/nn.3767 [PubMed: 25064852]

Campos CA, Bowen AJ, Roman CW, Palmiter RD, Encoding of danger by parabrachial CGRP neurons. Nature 555 (2018) pp. 617–622. 10.1038/nature25511 [PubMed: 29562230]

Campos CA, Bowen AJ, Schwartz MW, Palmiter RD, Parabrachial CGRP Neurons Control Meal Termination. Cell Metab. 23 (2016) pp. 811–820. 10.1016/j.cmet.2016.04.006 [PubMed: 27166945]

Carter ME, Han S, Palmiter RD, Parabrachial calcitonin gene-related peptide neurons mediate conditioned taste aversion. J. Neurosci. Off. J. Soc. Neurosci. 35 (2015) pp. 4582–4586. 10.1523/JNEUROSCI.3729-14.2015

Carter ME, Soden ME, Zweifel LS, Palmiter RD, Genetic identification of a neural circuit that suppresses appetite. Nature 503 (2013) pp. 111–114. 10.1038/nature12596 [PubMed: 24121436]

Chen JY, Campos CA, Jarvie BC, Palmiter RD, Parabrachial CGRP Neurons Establish and Sustain Aversive Taste Memories. Neuron 100 (2018) pp. 891–899 10.1016/j.neuron.2018.09.032 [PubMed: 30344042]

Chen Q, Ma K, Wang B, Chen Y, The possibility of alleviating chronic neuropathic pain and related behaviors by the direct suppression of the parabrachial nucleus. J. Clin. Neurosci. Off. J. Neurosurg. Soc. Australas. 95 (2022) pp. 180–187 10.1016/j.jocn.2021.11.019

Delamater AR, Treit D, Chlordiazepoxide attenuates shock-based and enhances LiCl-based fluid aversions. Learn. Motiv 19 (1988) pp. 221–238. 10.1016/0023-9690(88)90002-1

Douglass AM, Kucukdereli H, Ponserre M, Markovic M, Gründemann J, Strobel C, Alcala Morales PL, Conzelmann K-K, Lüthi A, Klein R, Central amygdala circuits modulate food consumption through a positive-valence mechanism. Nat. Neurosci. 20 (2017) pp. 1384–1394. 10.1038/nn.4623 [PubMed: 28825719]

Edvinsson JC, Reducha PV, Sheykhzade M, Warfvinge K, Haanes KA, Edvinsson L, Neurokinins and their receptors in the rat trigeminal system: Differential localization and release with implications for migraine pain. Mol. Pain 17 (2021) 10.1177/17448069211059400

Fenno LE, Mattis J, Ramakrishnan C, Hyun M, Lee SY, He M, Tucciarone J, Selimbeyoglu A, Berndt A, Grosenick L, Zalocusky KA, Bernstein H, Swanson H, Perry C, Diester I, Boyce FM, Bass CE, Neve R, Huang ZJ, Deisseroth K. Targeting cells with single vectors using multiple-feature Boolean logic. Nat Methods. 2014 Jul;11(7):763–72. doi: 10.1038/nmeth.2996. Epub 2014 Jun 8. [PubMed: 24908100]

Franceschini A, Costantini I, Pavone FS, Silvestri L, 2020. Dissecting Neuronal Activation on a Brain-Wide Scale With Immediate Early Genes. Front. Neurosci. 14 (2020) 10.3389/fnins.2020.569517

Freeman KB, Riley AL, The origins of conditioned taste aversion learning: A historical analysis, in: Conditioned Taste Aversion: Behavioral and Neural Processes. Oxford University Press, New York, NY, US, (2009) pp. 9–33.

Garcia J, Koelling RA, Relation of cue to consequence in avoidance learning. Psychon. Sci. 4 (1966) pp. 123–124.

Gemberling GA, Domjan M, Selective associations in one-day-old rats: taste-toxicosis and texture-shock aversion learning. J. Comp. Physiol. Psychol. 96 (1982) pp. 105–113. 10.1037/h0077855 [PubMed: 6276454]

Gemberling GA, Domjan M, Amsel A, Aversion learning in 5-day-old rats: taste-toxicosis and texture-shock associations. J. Comp. Physiol. Psychol. 94 (1980) pp. 734–745. 10.1037/h0077706 [PubMed: 7410632]

Guenthner CJ, Miyamichi K, Yang HH, Heller HC, Luo L, Permanent Genetic Access to Transiently Active Neurons via TRAP: Targeted Recombination in Active Populations. Neuron 78 (2013) pp. 773–784. 10.1016/j.neuron.2013.03.025 [PubMed: 23764283]

Gutierrez-Mecinas M, Bell AM, Marin A, Taylor R, Boyle KA, Furuta T, Watanabe M, Polgár E, Todd AJ, Preprotachykinin A is expressed by a distinct population of excitatory neurons in the mouse superficial spinal dorsal horn including cells that respond to noxious and pruritic stimuli. Pain 158 (2017) pp. 440–456. 10.1097/j.pain.0000000000000778 [PubMed: 27902570]

Han S, Soleiman MT, Soden ME, Zweifel LS, Palmiter RD, Elucidating an affective pain circuit that creates a threat memory. Cell 162 (2015) pp 363–374. doi: 10.1016/j.cell.2015.05.057 [PubMed: 26186190]

Holland PC, Wheeler DS, Representation-mediated food aversions, in: Conditioned Taste Aversion: Behavioral and Neural Processes. Oxford University Press, New York, NY, US, (2009) pp. 196–225.

Jia H-G, Zhang G-Y, Wan Q, A GABAergic projection from the central nucleus of the amygdala to the parabrachial nucleus: an ultrastructural study of anterograde tracing in combination with post-embedding immunocytochemistry in the rat. Neurosci. Lett. 382 (2005) pp. 153–157. [PubMed: 15911140]

Kang SJ, Liu S, Ye M, Kim D-I, Pao GM, Copits BA, Roberts BZ, Lee K-F, Bruchas MR, Han S, A central alarm system that gates multi-sensory innate threat cues to the amygdala. Cell Rep. 40 (2022) pp. 111222. 10.1016/j.celrep.2022.111222 [PubMed: 35977501]

Krane RV, Wagner AR, Taste aversion learning with a delayed shock US: Implications for the "generality of the laws of learning." J. Comp. Physiol. Psychol. 88 (1975) pp. 882–889. 10.1037/h0076417

Kronenberger JP, Médioni J. Food neophobia in wild and laboratory mice (Mus musculus domesticus). Behav Processes. 1985 Jun;11(1):53–9. doi: 10.1016/0376-6357(85)90102-0. [PubMed: 24924361]

Lee GJ, Kim YJ, Lee K, Oh SB, Patterns of brain c-Fos expression in response to feeding behavior in acute and chronic inflammatory pain condition. NeuroReport 32 (2021) pp. 1269–1277. 10.1097/WNR.0000000000001723 [PubMed: 34494992]

Lenzi SC, Cossell L, Grainger B, Olesen SF, Branco T, Margrie TW, Threat history controls flexible escape behavior in mice. Curr. Biol. CB 32 (2022) pp. 2972–2979 10.1016/j.cub.2022.05.022 [PubMed: 35659863]

Lundy R, Comparison of GABA, Somatostatin, and Corticotrophin-Releasing Hormone Expression in Axon Terminals That Target the Parabrachial Nucleus. Chem. Senses 45 (2020) pp. 275–282. 10.1093/chemse/bjaa010 [PubMed: 32107535]

Luskin AT, Bhatti DL, Mulvey B, Pedersen CE, Girven KS, Oden-Brunson H, Kimbell K, Blackburn T, Sawyer A, Gereau RW, Dougherty JD, Bruchas MR, Extended amygdala-parabrachial circuits alter threat assessment and regulate feeding. Sci. Adv. 7 (2021) 10.1126/sciadv.abd3666

Narushima M, Agetsuma M, Nabekura J, Development and experience-dependent modulation of the defensive behaviors of mice to visual threats. J. Physiol. Sci. JPS 72 (2022) 10.1186/s12576-022-00831-7

Palmiter RD, The Parabrachial Nucleus: CGRP Neurons Function as a General Alarm. Trends Neurosci. 41 (2018) pp. 280–293. 10.1016/j.tins.2018.03.007 [PubMed: 29703377]

Pauli JL, Chen JY, Basiri ML, Park S, Carter ME, Sanz E, McKnight GS, Stuber GD, Palmiter RD, Molecular and Anatomical Characterization of Parabrachial Neurons and Their Axonal Projections. Elife 11:e81868 eLife (2022) 10.7554/eLife.81868 [PubMed: 36317965]

Raver C, Uddin O, Ji Y, Li Y, Cramer N, Jenne C, Morales M, Masri R, Keller A, An Amygdalo-Parabrachial Pathway Regulates Pain Perception and Chronic Pain. J. Neurosci. Off. J. Soc. Neurosci. 40 (2020) pp. 3424–3442. 10.1523/JNEUROSCI.0075-20.2020

Roman C, Derkach V & Palmiter R Genetically and functionally defined NTS to PBN brain circuits mediating anorexia. Nat Commun 7, 11905 (2016). 10.1038/ncomms11905 [PubMed: 27301688]

Rusiniak KW, Palmerino CC, Rice AG, Forthman DL, Garcia J, Flavor-illness aversions: potentiation of odor by taste with toxin but not shock in rats. J. Comp. Physiol. Psychol. 96 (1982) pp. 527–539. 10.1037/h0077902 [PubMed: 6288778]

Sabatini PV, Frikke-Schmidt H, Arthurs J, Gordian D, Patel A, Rupp AC, Adams JM, Wang J, Beck Jørgensen S, Olson DP, Palmiter RD, Myers MG, Seeley RJ, GFRAL-expressing neurons suppress food intake via aversive pathways. Proc. Natl. Acad. Sci. 118 (2021) e2021357118. 10.1073/pnas.2021357118 [PubMed: 33593916]

Highlights

- Activation of Tac1^{PBN} neurons promotes escape, not freezing.
- Activation of Tac1^{PBN} neurons does not elicit conditioned taste aversion (CTA).
- Activation of Tac1^{PBN} neurons blocks CTA generated by LiCl or CGRP^{PBN} activation.
- Activation of Tac1+;CGRP− via INTRSECT replicates Tac1^{PBN} activation.

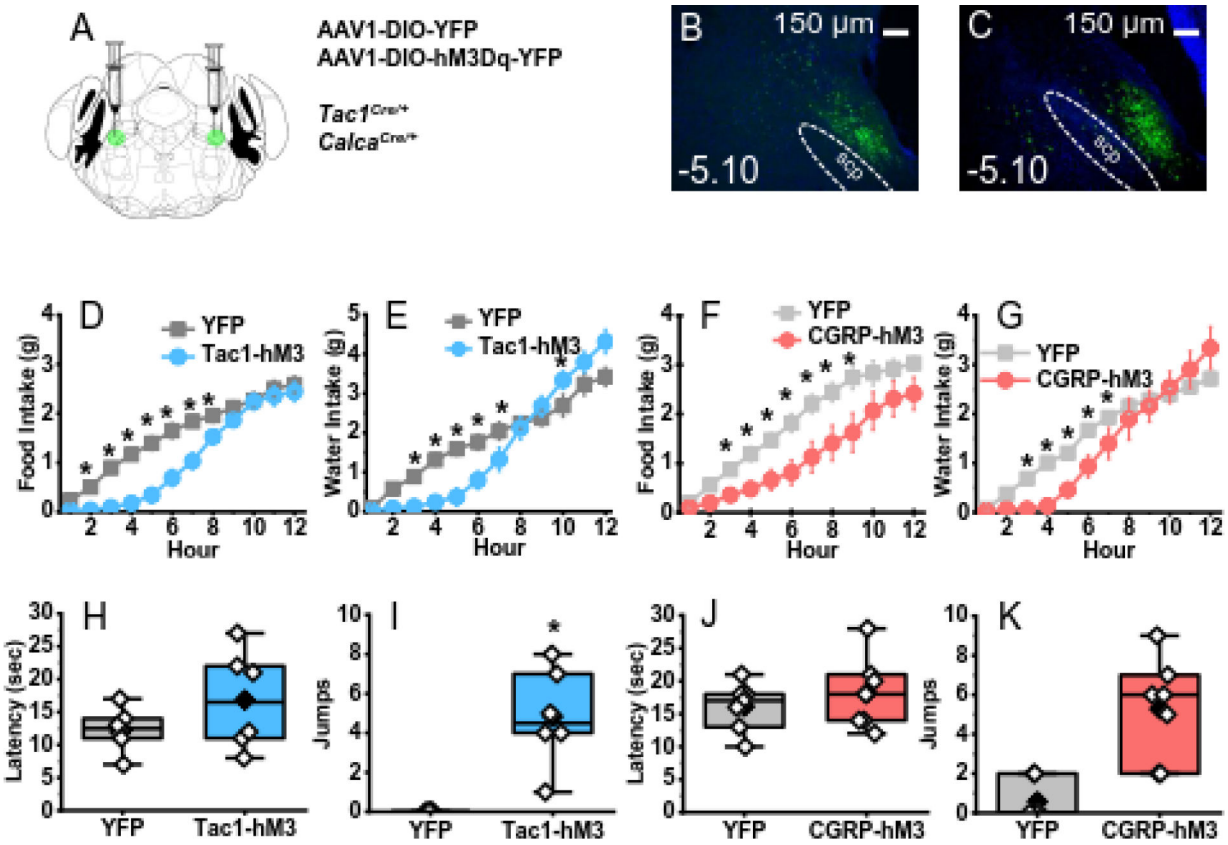

Figure 1. Chemogenetic activation of Tac1^{PBN} or CGRP^{PBN} neurons causes anorexia, adipsia, and jumping on a hotplate.

A) Schematic cartoon of stereotaxic viral injections of AAV1-DIO-YFP or AAV1-DIO-hM3Dq-YFP in the lateral PBN.

B) Representative image of a coronal section through PBN showing virus expression in *Tac1*$^{Cre/+}$ mouse.

C) Representative image of a coronal section through PBN showing virus expression in *Calca*$^{Cre/+}$ mouse.

D) Mice typically consume food throughout the dark cycle (Group YFP; n = 6); however, activating Tac1-hM3 (n = 7) neurons with CNO 30 min before the dark cycle results in robust anorexia.

E) As with food, mice consume water steadily throughout the dark cycle (Group YFP) and activation of Tac1^{PBN} neurons via CNO suppresses this intake (Group Tac1-hM3).

F) As previously demonstrated, activation of CGRP^{PBN} neurons (CGRP-hM3; n = 7) causes anorexia relative to YFP controls (n = 6).

G) CGRP-hM3 activation via CNO also causes adipsia.

H) When placed on a 55°C hotplate Tac1-hM3 activation does not cause a significant change to the latency to respond. (n = 6 per group)

I) Tac1-hM3 activation causes mice to jump off the hot plate repeatedly.

J) CGRP-hM3 activation does not alter the latency to respond to placement on a hot plate (n = 7 for both groups)

K) CGRP-hM3 activation causes mice to jump off the hotplate repeatedly. (n = 7 for both groups)

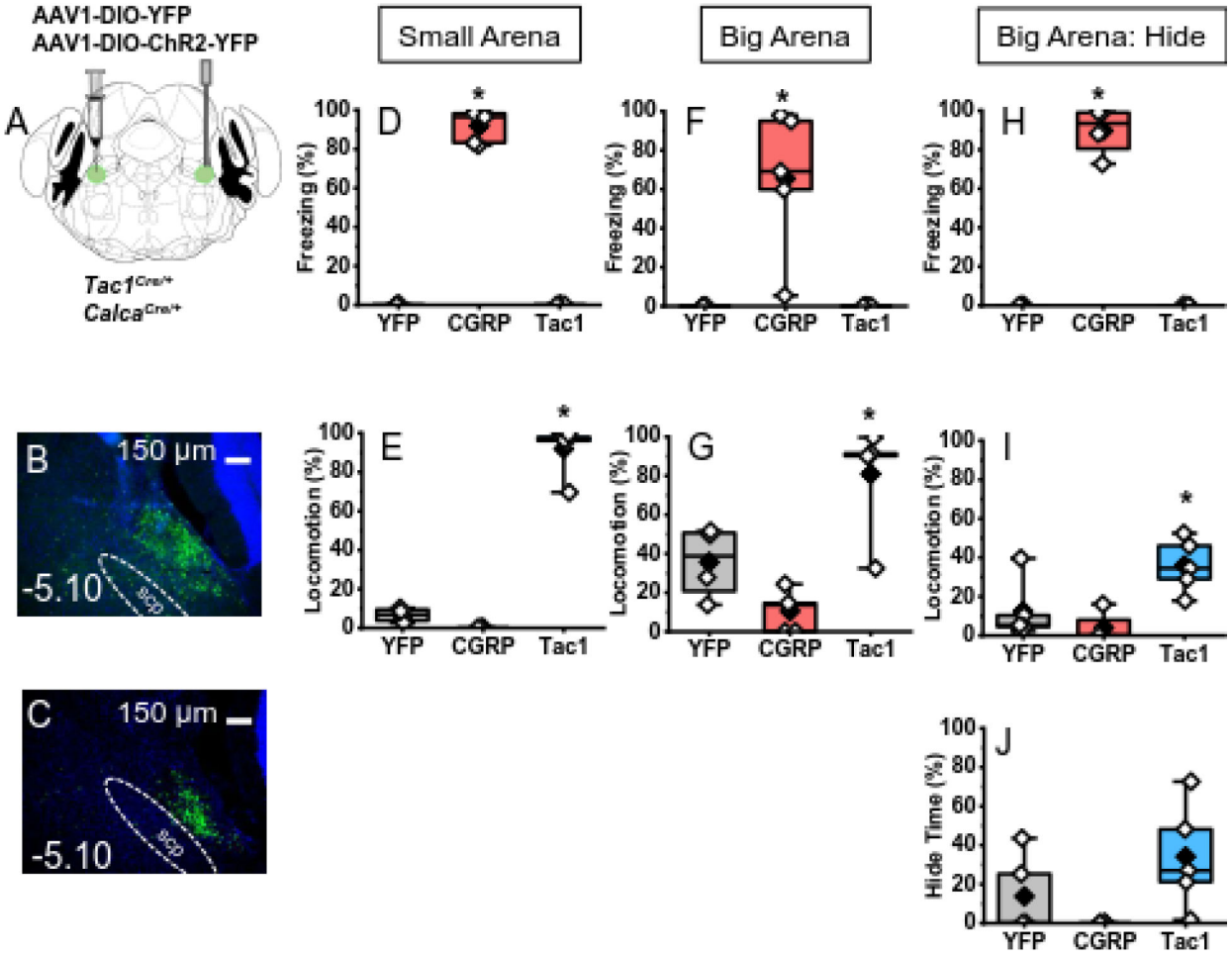

Figure 2. Optogenetic activation of Tac1^{PBN} or CGRP^{PBN} neurons elicits opposing defensive behaviors.

A) Schematic of viral injection and fiber optic cannula placement strategy targeting lateral PBN.

B) Representative 10X histological image from a Tac1$^{Cre/+}$ mouse showing viral expression and fiber placement.

C) Representative 10X histological image from a Calca$^{Cre/+}$ mouse showing viral expression and fiber placement.

D) Box and whisker plots of freezing (% of stimulation time) for YFP (n = 4), CGRP (n = 5), or Tac1 (n = 5) mice placed in a small (10×10 cm) arena.

E) Box and whisker plots of locomotion (% of stimulation time) for YFP (n = 4), CGRP (n = 5), or Tac1 (n = 5) mice placed in a small (10×10 cm) arena.

F) Box and whisker plots of freezing (% of stimulation time) for YFP (n =4), CGRP (n = 5), or Tac1 (n = 5) mice placed in a big (10×50 cm) arena.

G) Box and whisker plots of Locomotion (% of stimulation time) for YFP (n = 4), CGRP (n = 5), or Tac1 (n = 5) mice placed in a big (10×50 cm) arena.

H) Box and whisker plots of freezing (% of stimulation time) for YFP (n = 4), CGRP (n = 5), or Tac1 (n = 5) mice placed in a big (10×50 cm) arena with a partial hide box at one end (10×10 cm).

I) Box and whisker plots of locomotion (% of stimulation time) for YFP (n = 4), CGRP (n = 5), or Tac1 (n = 5) mice placed in a big (10×50 cm) arena with a partial hide box at one end (10×10 cm).

J) Box and whisker plots of hide time (% of stimulation time) for YFP (n = 4), CGRP (n = 5), or Tac1 (n = 5) mice placed in a big (10×50 cm) arena with a partial hide box at one end (10×10 cm).

Individual data points are represented as hollow diamonds, solid diamond indicates group means, the box represents the median, 25^{th}, and 75^{th} percentiles, and whiskers represent the 5^{th} and 95^{th} percentiles. Between-group differences indicated by significant between-group difference * $p < .05$.

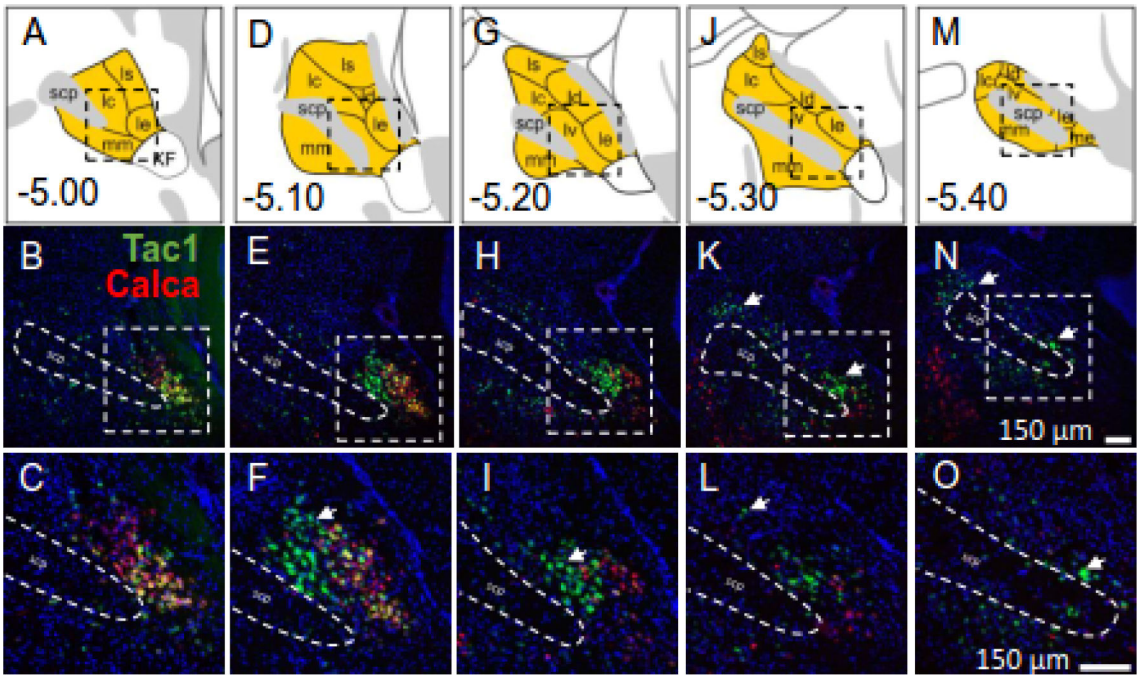

Figure 3. Distinct populations of neurons co-express Tac1 and Calca versus neurons that express Tac1 without Calca.

(A-C) Diagram of PBN subregions at −5.00 from Bregma based on the Allen Brain Atlas as well as representative histological images of $Tac1^{PBN}$ and $CGRP^{PBN}$ neurons at 10X and 20X.

(D-F) Diagram of PBN subregions at −5.10 from Bregma based on the Allen Brain Atlas as well as representative histological images of $Tac1^{PBN}$ and $CGRP^{PBN}$ neurons at 10X and 20X.

(G-I) Diagram of PBN subregions at −5.20 from Bregma based on the Allen Brain Atlas as well as representative histological images of $Tac1^{PBN}$ and $CGRP^{PBN}$ neurons at 10X and 20X.

(J-L) Diagram of PBN subregions at −5.30 from Bregma based on the Allen Brain Atlas as well as representative histological images of $Tac1^{PBN}$ and $CGRP^{PBN}$ neurons at 10X and 20X.

(M-O) Diagram of PBN subregions at −5.40 from Bregma based on the Allen Brain Atlas as well as representative histological images of $Tac1^{PBN}$ and $CGRP^{PBN}$ neurons at 10X and 20X.

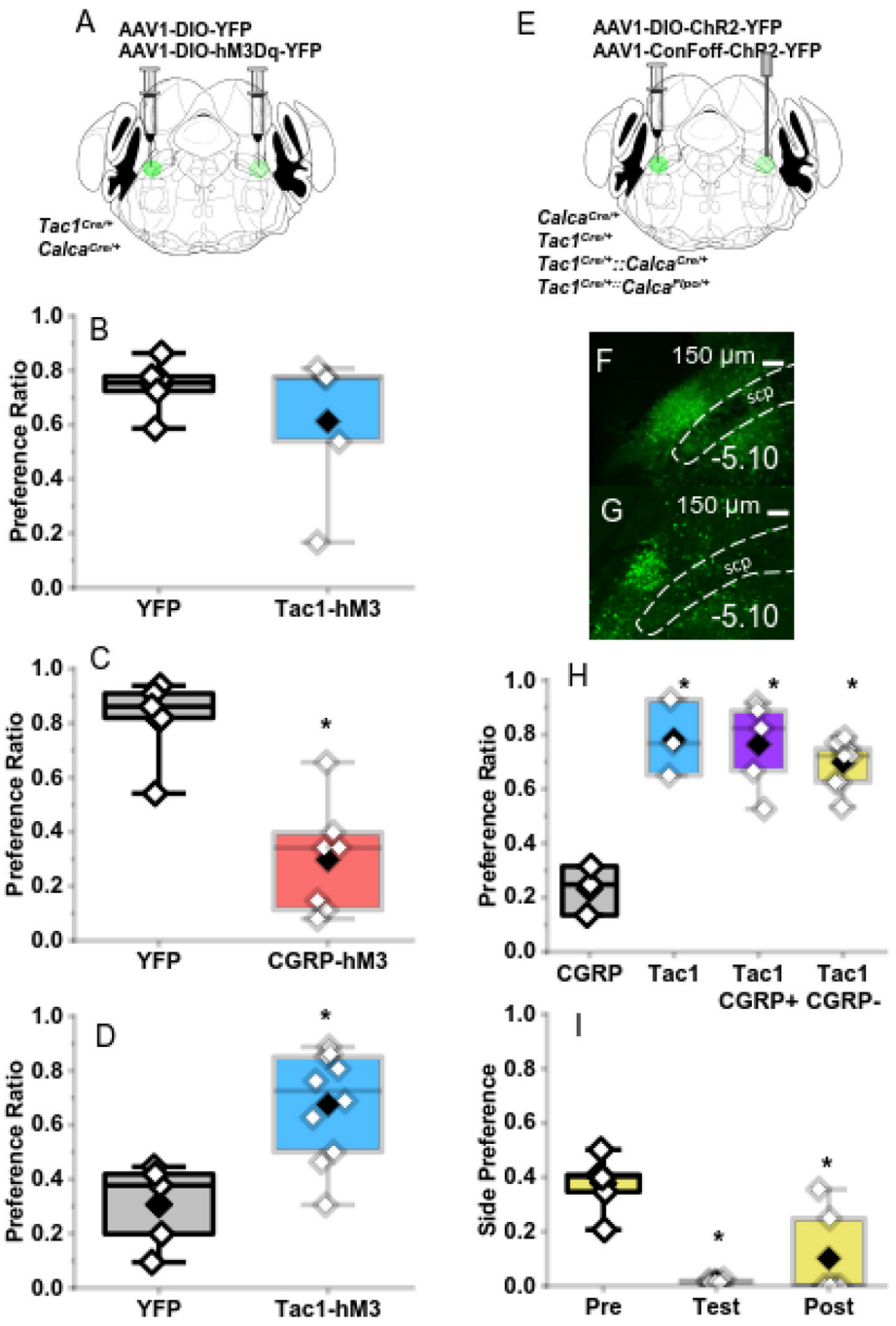

Figure 4. Activation of Tac1^{PBN} neurons suppresses conditioned taste aversion.

(A) Schematic diagram of viral injection targeting either AAV1-DIO-YFP or AAV1-DIO-hM3Dq-YFP to the lateral PBN of either *Tac1*$^{Cre/+}$ or *Calca*$^{Cre/+}$ mice.

(B) Pairing a novel tastant with activation of Tac1-hM3 neurons (n = 5) failed to generate a conditioned taste aversion (YFP, n = 6).

(C) Pairing a novel tastant with activation of CGRP-hM3 neurons (n = 7) caused a significant conditioned taste aversion. (YFP n = 5)

(D) Activation of Tac1-hM3 neurons (n = 10) just after the consumption of a novel taste but 30-min before the administration of LiCl attenuated the conditioned taste aversion as compared to YFP mice (n = 5) that learned a significant taste aversion.

(E) Schematic diagram of viral injection and fiber optic targeting of either AAV1-DIO-ChR2-YFP or AAV1-ConFoff-ChR2-YFP in either *Tac1*$^{Cre/+}$, *Calca*$^{Cre/+}$, *Tac1*$^{Cre/+}$*::Calca*$^{Cre/+}$, or *Tac1*$^{Cre/+}$*::Calca*$^{Flpo/+}$ mice.

(F) Representative image of a coronal section through PBN showing virus expression in *Tac1Cre/+::Calca*$^{Cre/+}$ mouse.

(G) Representative image of a coronal section through PBN showing virus expression in *Tac1*$^{Cre/+}$*::Calca*$^{Flpo/+}$ mouse.

(H) Activation of CGRP (n = 3) neurons produced a robust CTA; however, activation of either Tac1 neurons (n = 3), Tac1 and CGRP neurons (i.e., Tac1$^{Cre/+}$::Calca$^{Cre/+}$ mice injected with AAV1-DIO-ChR2-YFP; n = 5), or Tac1+CGRP− neurons (i.e., Tac1$^{Cre/+}$::Calca$^{Flpo/+}$ mice injected with AAV1-ConFoff-ChR2-YFP; n = 9) failed to generate a CTA.

(I) Activation of Tac1+CGRP− neurons (n = 6) resulted in avoidance during a real-time place preference paradigm.

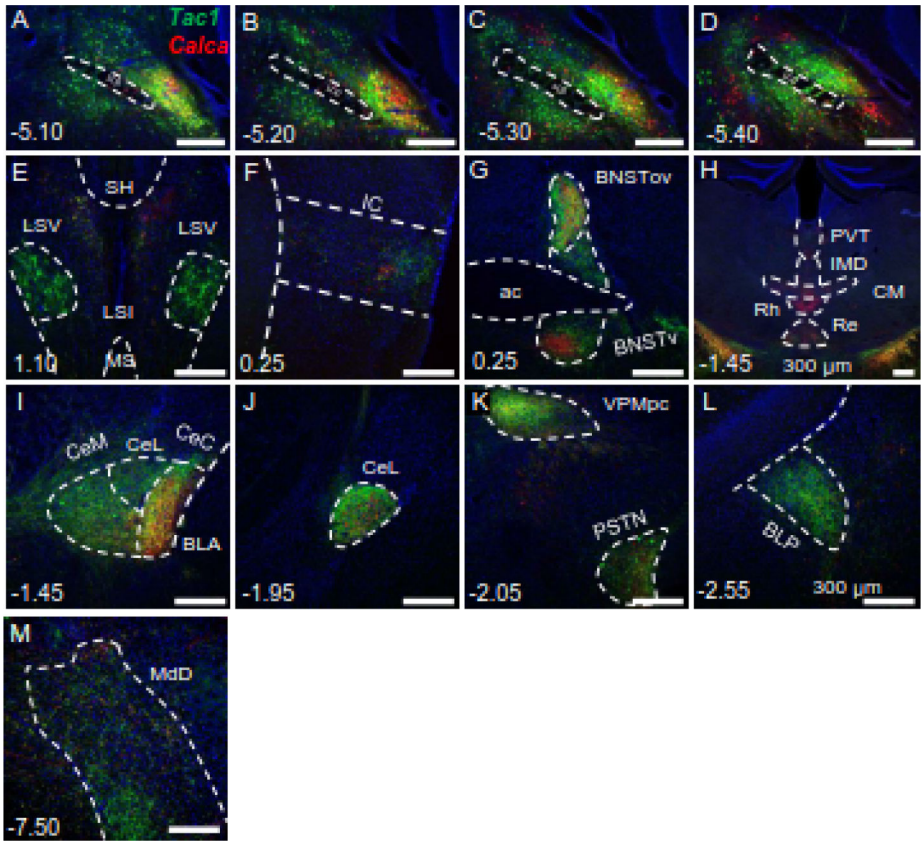

Figure 5. Tac1+CGRP–^{PBN} and CGRP^{PBN} neurons project axons to distinct brain regions

(A-D) Four coronal sections of PBN neurons expressing Tac1 (green), CGRP (red), or both (yellow) from rostral to caudal at −5.10 mm caudal to bregma (A) −5.20 mm caudal to bregma (B) −5.30 mm caudal to bregma (C) and −5.40 mm caudal to bregma (D). Dashed white line highlights the scp.

(E) Fibers in the lateral septum around 1.10 mm rostral to bregma.

(F) Fibers in the insular cortex around 0.25 mm rostral to bregma.

(G) Fibers in BNST about 0.25 mm rostral to bregma.

(H) Fibers in the thalamus about −1.45 mm caudal to bregma.

(I) Fibers in the middle of CeA about −1.45 mm caudal to bregma.

(J) Fibers in caudal CeA at about −1.95 mm caudal to bregma.

(K) Fibers in the VPMpc and PSTN at about −2.05 mm caudal to bregma.

(L) Fibers in the posterior part of the basolateral amygdala (BLP) at about −2.55 mm from bregma. All scale bars represent 300 μm.

(M) 2X image of fibers in the medulla including the medullary reticular nucleus dorsal part (MdD) at about −7.30 mm from bregma. The nucleus ambiguous (na) is outlined as a reference point.